

# Analysis of positive and negative triangularity L-mode plasmas by SOLPS-ITER modelling

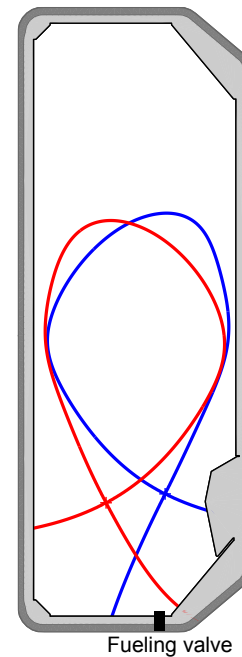
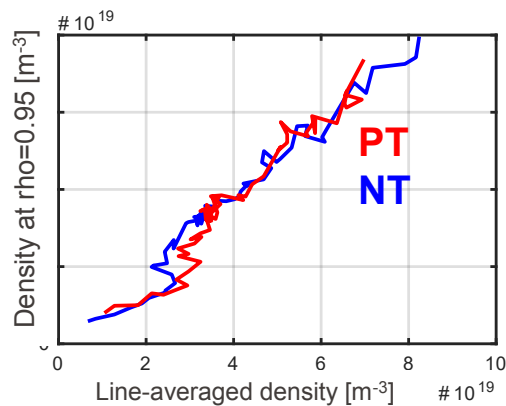
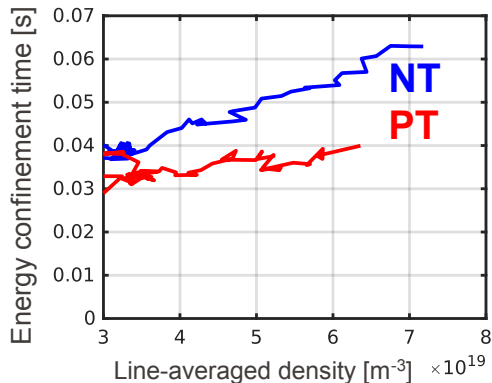
Elena Tonello

F. Mombelli, M. Passoni, O. Février, S. Gorno, P. Ricci, T. Bolzonella, N. Vianello

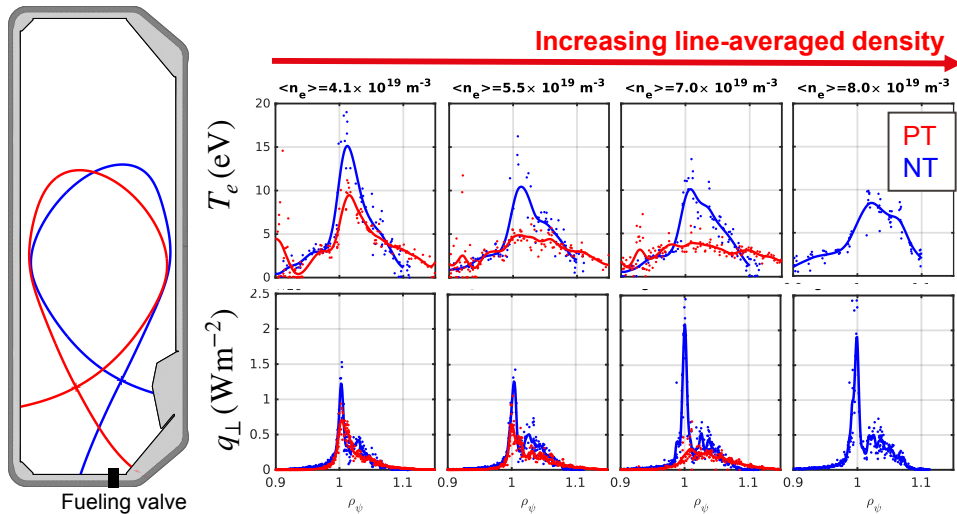


- **Motivation:** L-mode detachment experiments in TCV - PT vs. NT
- **The SOLPS-ITER code**
  - Physics, equations and geometry
  - Simulation setup and strategy
- **Results**
  - Reference simulation: attached condition and benchmark with experiments
  - Density ramp trends
- **Conclusions and perspectives**

- L-Mode,  $I_p = 220\text{kA}$ , Ohmic heating only
- Configuration mirrored around  $R_0=0.88\text{ m}$ :
  - Negative triangularity (**NT**):  $\delta_{\text{top}} = -0.30$  and  $\delta_{\text{bot}} = -0.27$
  - Positive triangularity (**PT**):  $\delta_{\text{top}} = 0.27$  and  $\delta_{\text{bot}} = 0.29$
- In core density rumps, for the same fueling rate,  $\langle n_e \rangle_{\text{NT}} > \langle n_e \rangle_{\text{PT}}$  while  $n_{e,\text{sep,NT}} \simeq n_{e,\text{sep,PT}}$



[O. Février, Invited EPS 2023]



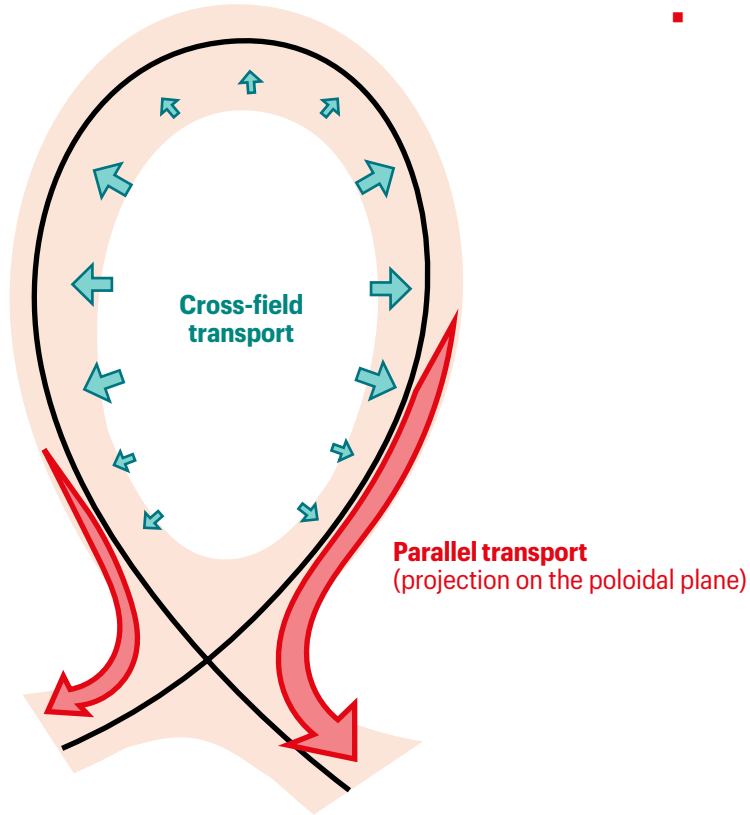
- **Reduction** of the OSP  $T_e$  and heat flux **in PT**, but **not in NT**
- Indication of **reduced OSP detachment in NT** with respect to PT

[O. Février, Invited EPS 2023]

The aim of the simulations is to **interpret** these results in light of **SOLPS-ITER** modelling

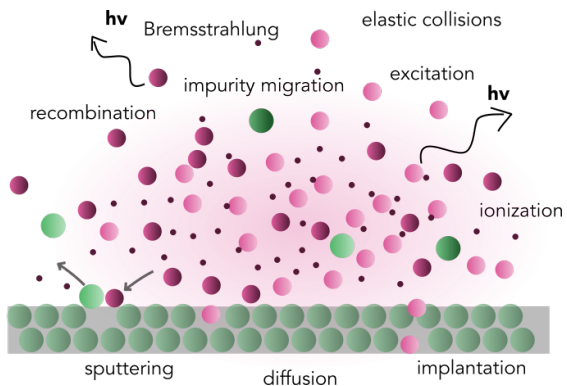
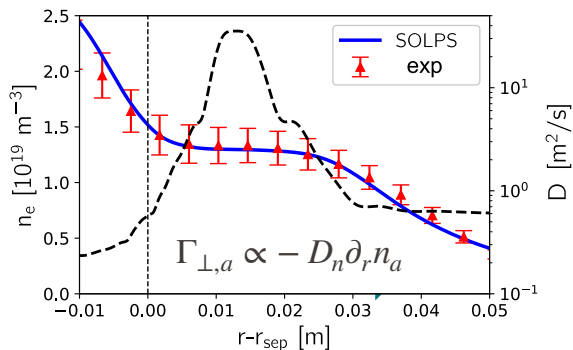


- Motivation: L-mode detachment experiments in TCV - PT vs. NT
- **The SOLPS-ITER code**
  - Physics, equations and geometry
  - Simulation setup and strategy
- **Results**
  - Reference simulation: attached condition and benchmark with experiments
  - Density ramp trends
- **Conclusions and perspectives**



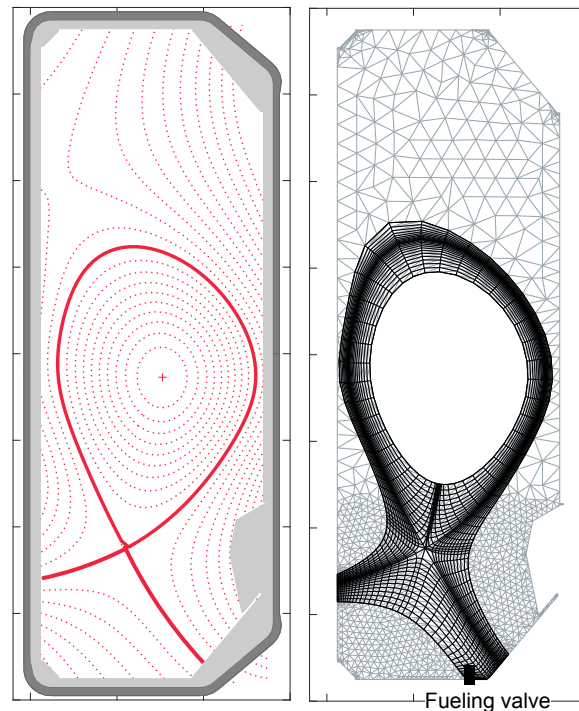
- Model the **main mechanisms controlling power exhaust** in tokamaks and quantitatively **estimate fluxes** on the PFCs
  - time scale  $\sim 1$ s
  - full size device up to DEMO scale

[P. Mantz et al. Phys. Plasmas 27, 022506 (2020)]

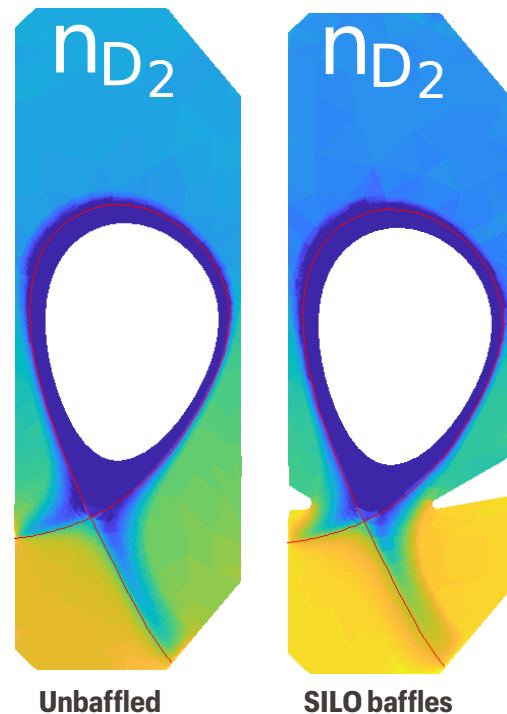


- Model the **main mechanisms controlling power exhaust** in tokamaks and quantitatively **estimate fluxes** on the PFCs
  - time scale  $\sim 1$ s
  - full size device up to DEMO scale
  
- **Cross-field transport:**
  - Poloidal and cross field contributions due to drifts may also be included
  - The average effect of turbulence as diffusive process controlled by  $D_n, \chi_{e,i}$
  
- **Plasma-neutral interaction and plasma-wall interaction:**
  - Poloidal and cross field contributions due to drifts may also be included

- 2D model: computational domain in the **poloidal plane** (2.5D if drifts are on: it includes effects of  $B_\phi$ )
- **Field-aligned plasma mesh:**
  - Generated on the experimental magnetic equilibrium reconstruction
  - Extend up to the first open flux-surface touching the wall



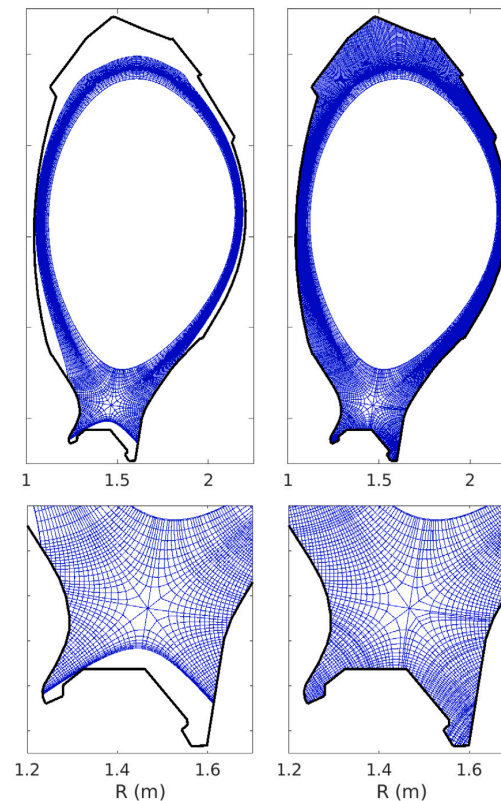
- 2D model: computational domain in the **poloidal plane** (2.5D if drifts are on: it includes effects of  $B_\phi$ )
- **Field-aligned** plasma mesh:
  - Generated on the experimental magnetic equilibrium reconstruction
  - Extend up to the first open flux-surface touching the wall
- Flexibility of **Monte Carlo geometry**: neutral injection, recycling and sputtering, divertor closure



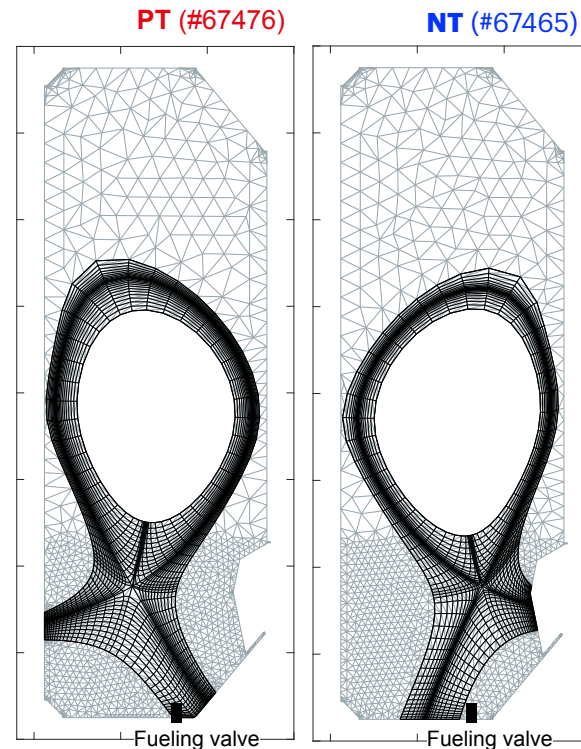
[M. Wensing PhD thesis, 2021]

- 2D model: computational domain in the **poloidal plane** (2.5D if drifts are on: it includes effects of  $B_\phi$ )
- **Field-aligned** plasma mesh:
  - Generated on the experimental magnetic equilibrium reconstruction
  - Extend up to the first open flux-surface touching the wall
- Flexibility of **Monte Carlo geometry**: neutral injection, recycling and sputtering, divertor closure
- Now possible to **extend plasma grid** all over the vessel (not used in this work)

[W. Dekeyser et al, NME 2021]



- Computational meshed built on PT and NT experimental equilibria: **same poloidal and radial resolution**.
- NT and PT simulations are performed at **fixed input parameters**: assess the effect of different plasma meshes
  - $P_{\text{in,e}} = P_{\text{in,i}} = 0.5 \times (P_{\text{Ohm}} - P_{\text{rad,core}}) \simeq 100 \text{ kW}$
  - Upstream density:  $n_{e,\text{sep}} = 1.0 \times 10^{19} \text{ m}^{-3}$
- No drifts, D only (neglect C impurities)

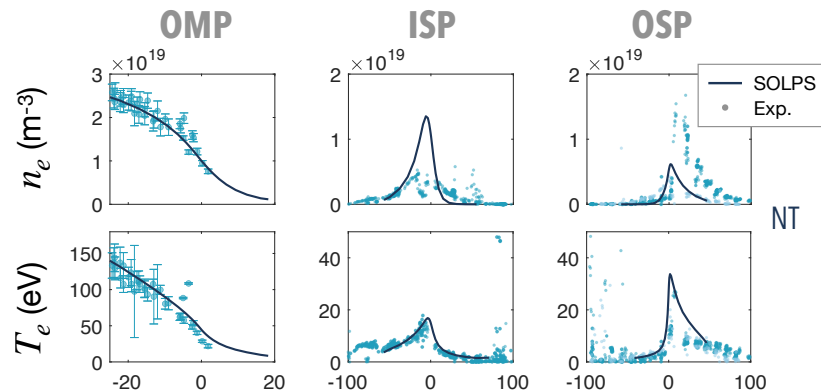


- Motivation: L-mode detachment experiments in TCV - PT vs. NT
- **The SOLPS-ITER code**
  - Physics, equations and geometry
  - Simulation setup and strategy
- **Results**
  - Reference simulation: attached condition and validation with experiments
  - Density ramp trends
- **Conclusions and perspectives**

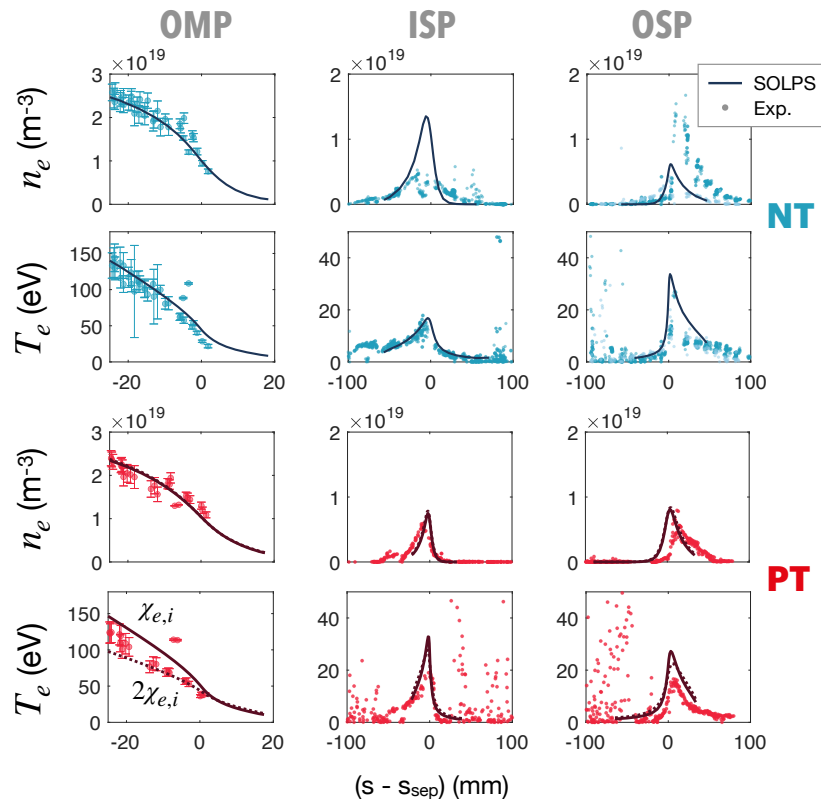


- $D_n$  and  $\chi_{e,i}$  optimised for NT and kept fixed switching to PT

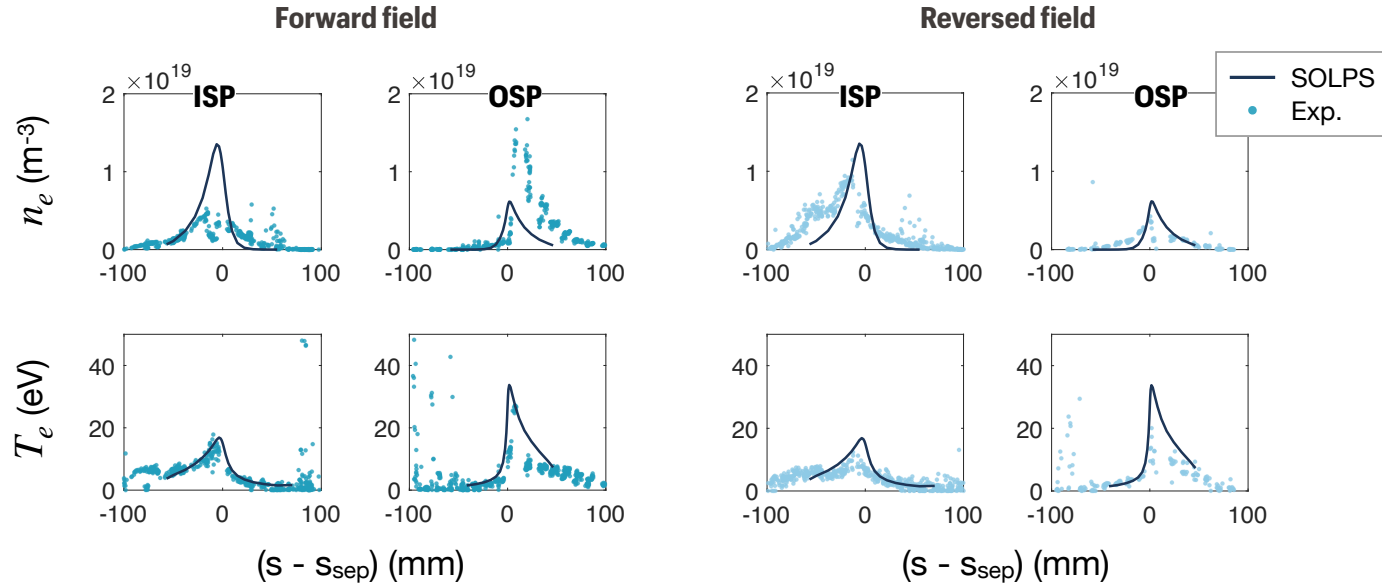
- $D_n = 0.2 \text{ m}^2\text{s}^{-1}, \chi_{e,i} = 1.0 \text{ m}^2\text{s}^{-1}$



- $D_n$  and  $\chi_{e,i}$  optimised for NT and kept fixed switching to PT
  - $D_n = 0.2 \text{ m}^2\text{s}^{-1}, \chi_{e,i} = 1.0 \text{ m}^2\text{s}^{-1}$
- In **agreement** with experiments:
  - Overall agreement, both for NT and PT
  - $T_{e,\text{max}@\text{OSP}} > T_{e,\text{max}@\text{ISP}}$  in NT and  
 $T_{e,\text{max}@\text{OSP}} \simeq T_{e,\text{max}@\text{ISP}}$  in PT (...effect of connection length?)
- Discrepancies:**
  - $n_e$  profiles at the target in NT (...drifts?)
  - Overestimation of upstream  $T_e$  profile if PT, agreement improves if  $\chi_{e,\text{NT}} > \chi_{e,\text{PT}}$  (lower energy confinement..?)



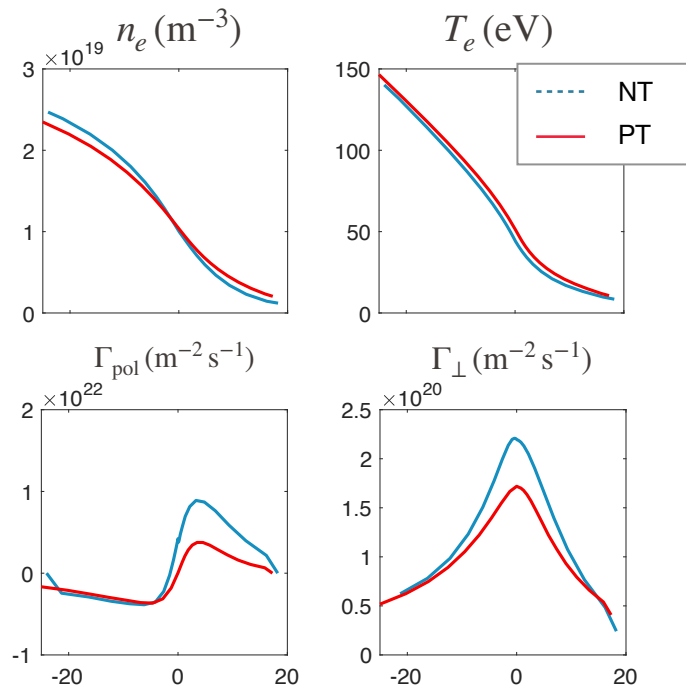
- Field reversal has significant effect on the target  $n_e$  profiles, while  $T_e$  is almost unaffected
- To analyse the effect of field reversal with SOLPS-ITER drifts need to be included



Steady state density equation:  $\nabla \cdot (\vec{\Gamma}) = S_n$

■ OMP profiles:

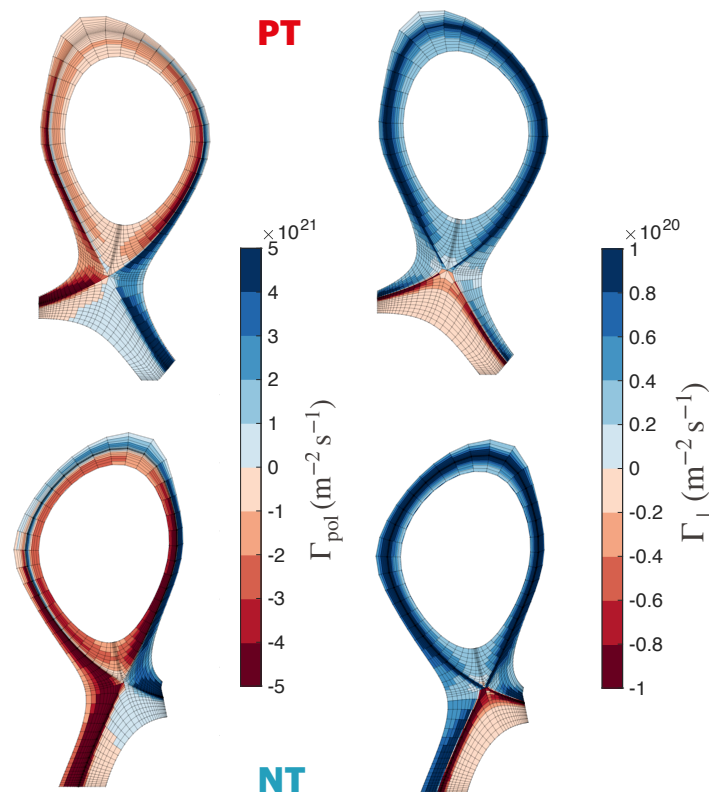
- for the same  $n_{e,sep}$ ,  $|\partial_r n_e| >$  in NT than PT
- since  $D_n = 0.2 \text{ m}^{-2} \text{ s}^{-1}$  (same for both),  $\Gamma_{\perp} >$  in NT than PT
- $\Gamma_{pol} >$  in NT than PT



Steady state density equation:  $\nabla \cdot (\vec{\Gamma}) = S_n$

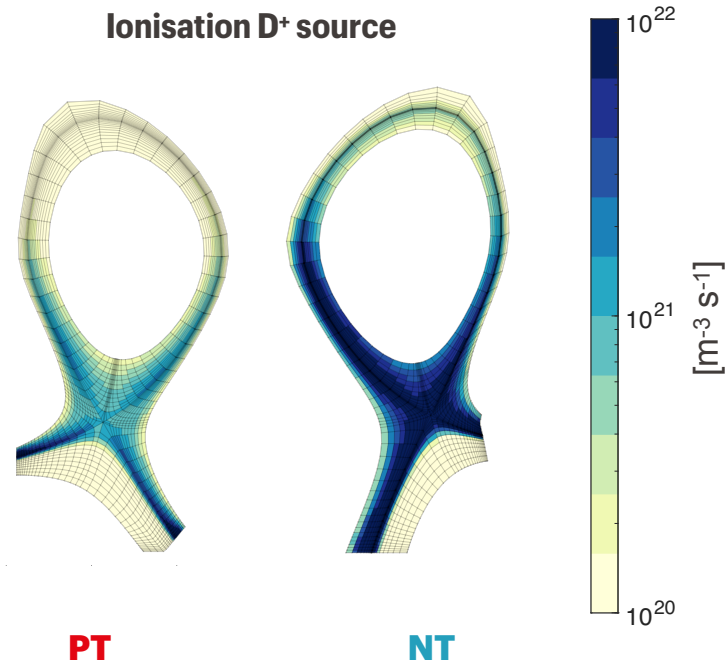
■ OMP profiles:

- for the same  $n_{e,sep}$ ,  $|\partial_r n_e| >$  in NT than PT
- since  $D_n = 0.2 \text{ m}^{-2}\text{s}^{-1}$  (same for both),  $\Gamma_{\perp} >$  in NT than PT
- $\Gamma_{pol} >$  in NT than PT
- positive  $\Gamma_{pol}$  (clockwise in the poloidal plane) to higher field region in NT

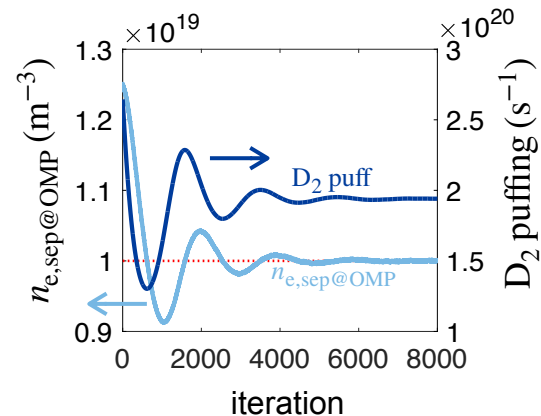


Steady state density equation:  $\nabla \cdot (\vec{\Gamma}) = S_n$

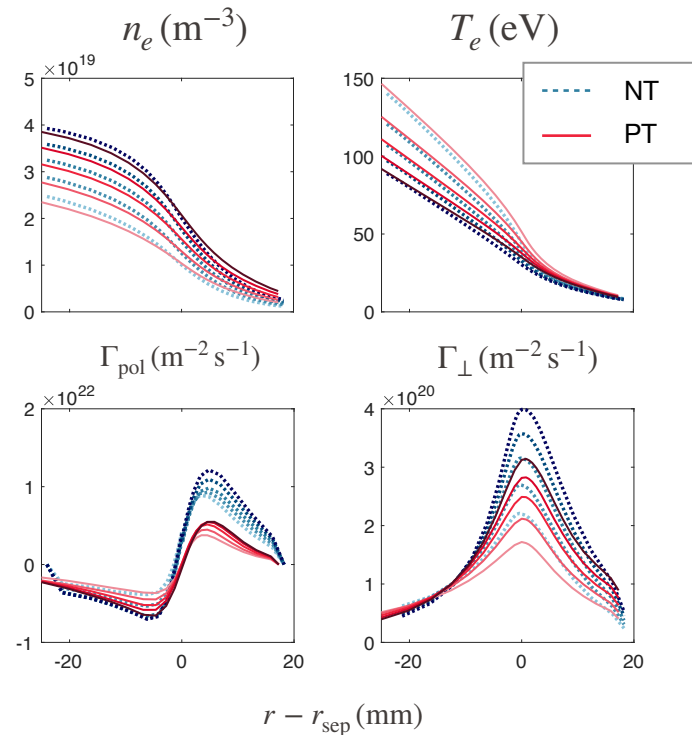
- **OMP profiles:**
  - for the same  $n_{e,sep}$ ,  $|\partial_r n_e| >$  in NT than PT
  - since  $D_n = 0.2 \text{ m}^{-2}\text{s}^{-1}$  (same for both),  $\Gamma_{\perp} >$  in NT than PT
  - $\Gamma_{pol} >$  in NT than PT
  - positive  $\Gamma_{pol}$  (clockwise in the poloidal plane) to higher field region in NT
- **Ionisation distribution** is also different in NT and PT: ~factor 5 higher in NT!



- Density ramp as a  $n_{e,sep}$  scan in SOLPS-ITER
- SOLPS-ITER density scan using the **density feedback scheme**:  $D_2$  influx is adjusted iteratively to match specified  $n_{e,sep}$
- Six simulations, repeated for PT and NT:  
 $n_{e,sep} = \{ 0.75 - 1.00 - 1.25 - 1.50 - 1.75 - 2.0 \} \times 10^{19} \text{ m}^{-3}$
- Fixed anomalous transport and input power

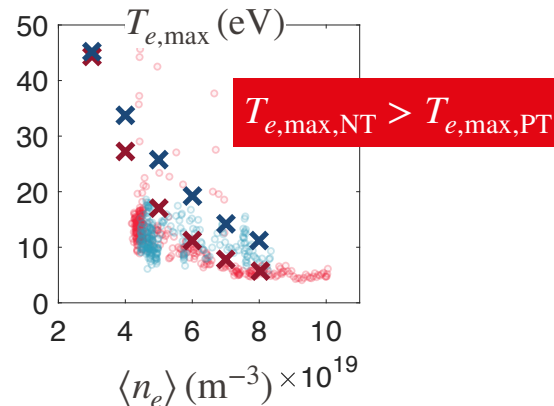
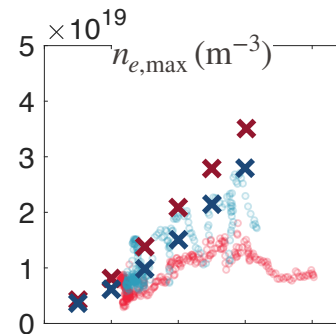


- Density ramp, i.e. increase of  $n_e$  at the core boundary, obtained by reducing  $D_n$
- Stronger effect on  $\Gamma_{\perp}$ , for increasing  $n_{e,\text{core}}$ 
  - increasing  $n_{e,\text{sep}}$ ,  $\Gamma_{\perp}$  increases
  - decreasing  $D_n$ ,  $\Gamma_{\perp} \propto D_n$  decreases



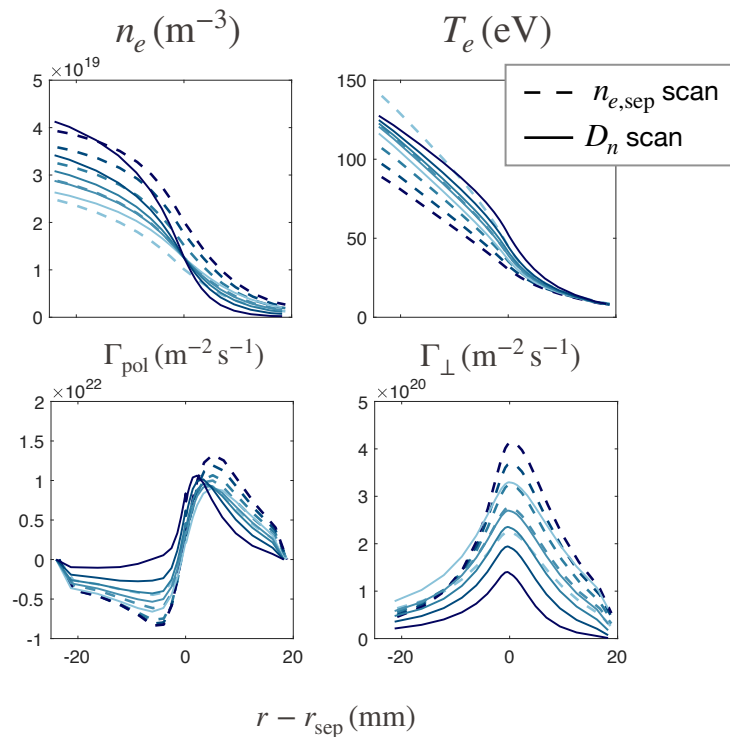


- Density ramp, i.e. increase of  $n_e$  at the core boundary, obtained by reducing  $D_n$
- Stronger effect on  $\Gamma_{\perp}$ , for increasing  $n_{e,\text{core}}$ 
  - increasing  $n_{e,\text{sep}}$ ,  $\Gamma_{\perp}$  increases
  - decreasing  $D_n$ ,  $\Gamma_{\perp} \propto D_n$  decreases
- Simulations **predicts the experimental trend** of higher OSP  $T_e$  in NT compared to PT
- Flux roll-over in PT is not observed in simulations



# Density ramp: $n_{e,sep}$ scan vs. $D_n$ scan

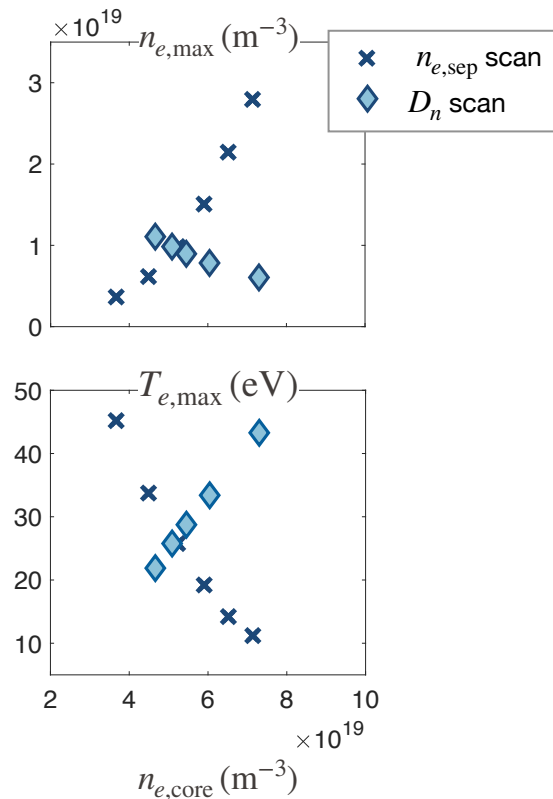
- Density ramp, i.e. increase of  $n_e$  at the core boundary, obtained by reducing  $D_n$
- Stronger effect on  $\Gamma_{\perp}$ , for increasing  $n_{e,core}$ 
  - increasing  $n_{e,sep}$ ,  $\Gamma_{\perp}$  increases
  - decreasing  $D_n$ ,  $\Gamma_{\perp} \propto D_n$  decreases



# Density ramp: $n_{e,sep}$ scan vs. $D_n$ scan

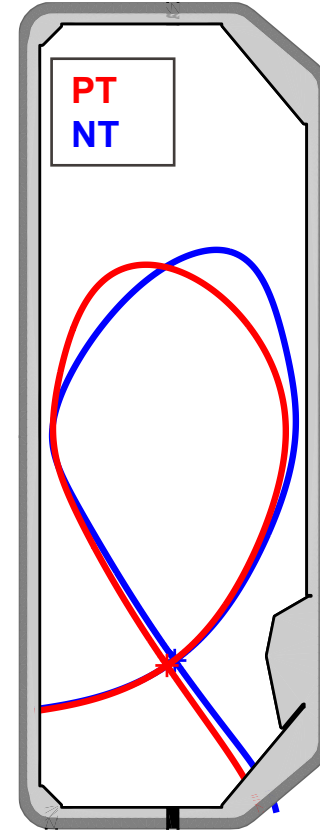
- Density ramp, i.e. increase of  $n_e$  at the core boundary, obtained by reducing  $D_n$
- Stronger effect on  $\Gamma_{\perp}$ , for increasing  $n_{e,core}$ 
  - increasing  $n_{e,sep}$ ,  $\Gamma_{\perp}$  increases
  - decreasing  $D_n$ ,  $\Gamma_{\perp} \propto D_n$  decreases
- Effects at the **OSP**:
  - increasing  $n_{e,sep}$ ,  $T_{e,max}$  decreases and  $n_{e,max}$  increases
  - decreasing  $D_n$ ,  $T_{e,max}$  increases and  $n_{e,max}$  decreases

OSP trends

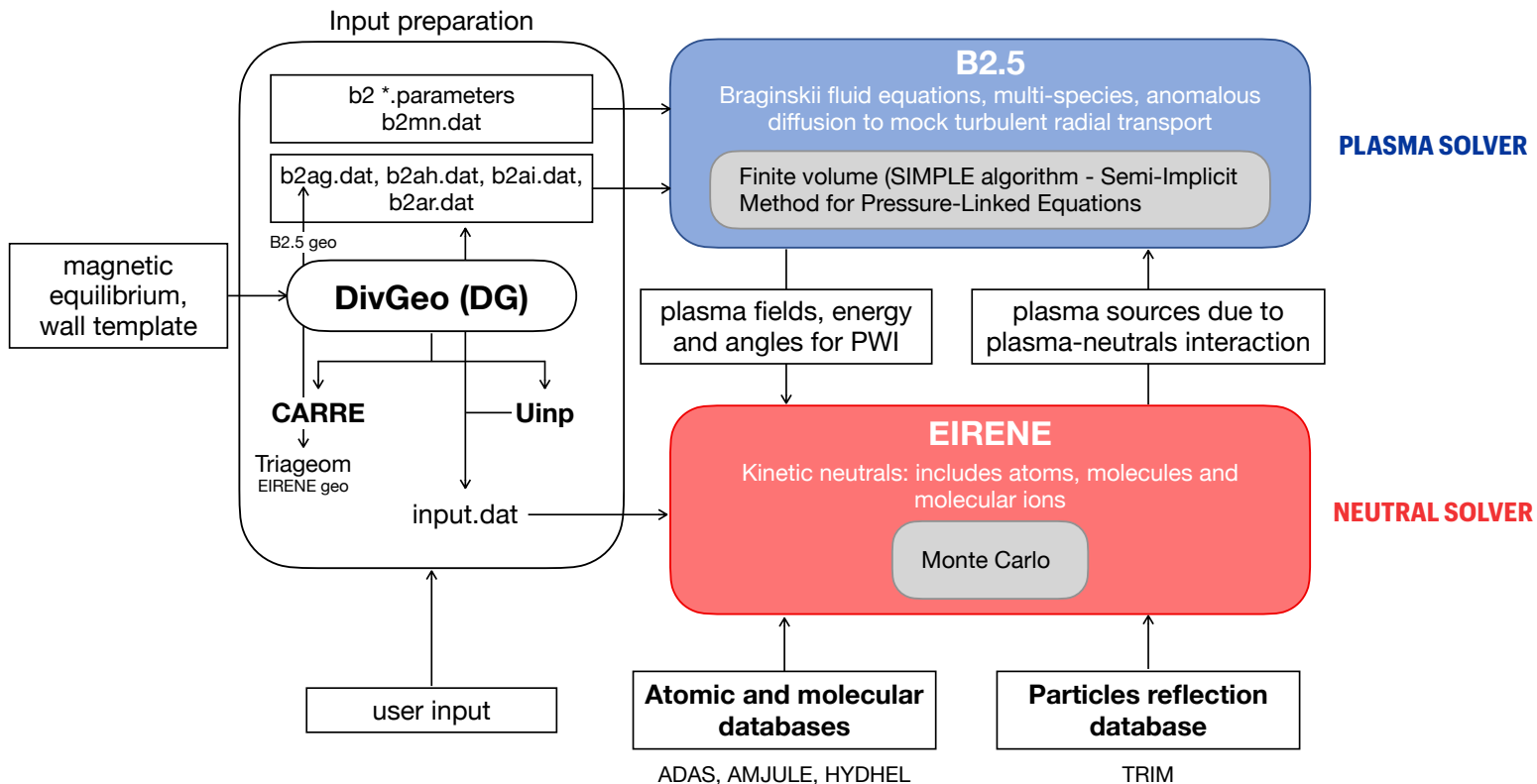


- Comparison of PT and NT TCV L-mode shots by SOLPS-ITER modelling
- **Validation** of the simulation in attached condition for NT:
  - Keeping the same input parameters (including radial transport), good agreement also with PT profile
  - Differences in radial and poloidal fluxes and particle sources although same input parameters
- Trends during **density ramp**:
  - Simulations predict higher OSP  $T_e$  in NT compared to PT
  - ~constant OSP  $T_e$  observed experimentally in NT, may be connected to a reduction of radial transport

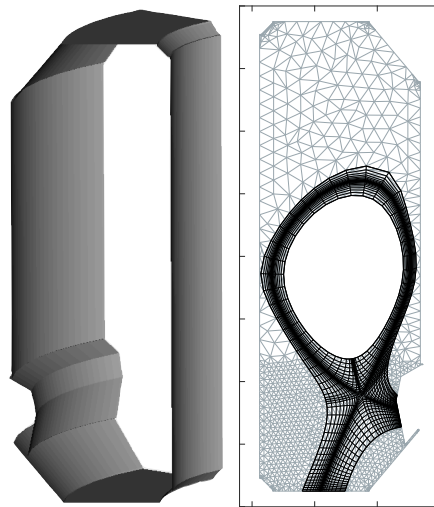
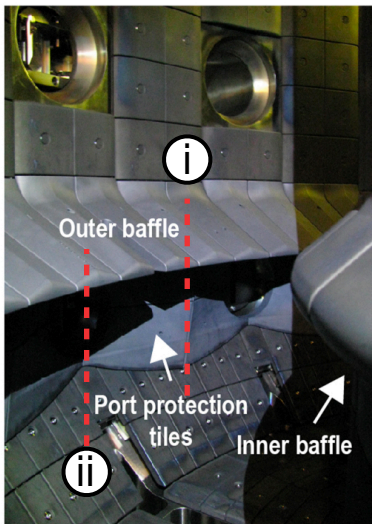
- **Priority:** isolate the effect of connection length ( $L_{\parallel}$ ) by modelling NT and PT with the same diverter geometry
  - include drifts..
  - include C impurities...



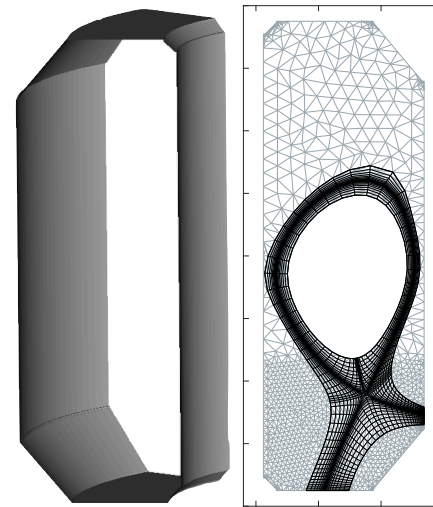
# Backup slides



[H. Reimerdes et al/ 2021 Nucl.  
Fusion 61 024002]



**i** Toroidal symmetric port protection tiles



**ii** No port protection tiles



- Narrower  $T_e$  profiles at the OSP, no differences in  $T_{e,max}$

